



Bilayer Stabilized Ln³⁺-doped CaMoO₄ Nanocrystals with High Luminescence Quantum Efficiency and Photocatalytic Properties

Journal:	<i>Dalton Transactions</i>
Manuscript ID:	DT-COM-12-2013-053450.R1
Article Type:	Communication
Date Submitted by the Author:	16-Jan-2014
Complete List of Authors:	Mahalingam, Venkataramanan; Indian Institute of Science Education and Research (IISER) Kolkata, Mohanpur Campus Hazra, Chanchal; Indian Institute of Science Education and Research (IISER)-Kolkata, Chemical Sciences Samanta, Tuhin; Indian Institute of Science Education and Research (IISER)-Kolkata, Chemical Sciences Asaithambi, Aswin; Indian Institute of Science Education and Research (IISER)-Kolkata, Chemical Sciences

ARTICLE

Bilayer Stabilized Ln^{3+} -doped CaMoO_4 Nanocrystals with High Luminescence Quantum Efficiency and Photocatalytic Properties

Cite this: DOI: 10.1039/x0xx00000x

Received 00th January 2012,
Accepted 00th January 2012

DOI: 10.1039/x0xx00000x

www.rsc.org/

Chanchal Hazra, Tuhin Samanta, Aswin Vijai Asaithambi and Venkataramanan Mahalingam*

In this article we discuss the microwave synthesis of sodium dodecyl sulphate (SDS) stabilized Ln^{3+} -doped CaMoO_4 nanocrystals ($\text{Ln}^{3+} = \text{Eu}^{3+}, \text{Er}^{3+}/\text{Yb}^{3+}$). The nanocrystals are quite monodispersed with average size close to 100 nm. FTIR and TGA analyses suggest the strong binding of SDS molecules to the CaMoO_4 nanocrystals surface. The high dispersibility of the nanocrystals in water implies that SDS stabilizes the nanocrystals as bilayer structure. The SDS coating also assists in the easy dispersion of the nanocrystals in toluene without any additional surface chemistry. The Eu^{3+} ions doped in CaMoO_4 nanocrystals display very strong red luminescence with a quantum yield close to 40%. Under 980 nm excitation, $\text{Er}^{3+}/\text{Yb}^{3+}$ -doped CaMoO_4 nanocrystals display Er^{3+} emissions at 550 and 650 nm. In addition, interestingly, a NIR peak around 833 nm is observed which occurred via a three photon process. Furthermore, CaMoO_4 nanocrystals exhibit photocatalytic activity which is studied through degradation of Rhodamine B (RhB) dye in neutral condition. The RhB dye is significantly degraded by ~80% under UV illumination within 4 hrs and the rate of degradation is comparable to that observed for well known ZnO nanoparticles. The high luminescence quantum efficiency and strong photocatalytic activity of Ln^{3+} -doped CaMoO_4 nanocrystals make them a potential material for dual applications such as bio-imaging and photocatalyst.

1 Introduction

Lanthanide (Ln^{3+})-doped luminescent nanomaterials are continuously drawing much attention due to their characteristic sharp transitions arising from inner $4f$ orbitals. The sharp transition is due to shielding of $4f$ orbitals by $5s$ and $5p$ orbitals.¹ These transitions have low absorption coefficients due to parity forbidden, resulting in the long luminescence lifetime from μs to ms region.² Intra $4f$ transitions are narrow and occur over a wide spectral region (from ultraviolet to near infrared) and find potential advantages for use in colour displays due to high colour purity, phosphors, and bio-marking applications.³ In addition to the Stokes emission, these Ln^{3+} ions possess several energy levels which are close enough to convert the lower energy radiation to the higher energy visible emission, a process well known as upconversion luminescence.⁴

Recently there has been an increasing demand for water dispersible Ln^{3+} -doped nanocrystals due to their potential use as bioprobes.⁵ Most of the studies in this area are mainly focussed towards developing Ln^{3+} -doped fluoride nanocrystals partly due to their ease in synthesis as well as the availability of a range of synthetic procedures.⁶⁻⁸ However, studies on water dispersible oxide-based materials such as oxides, vanadates, phosphates, sulphates, molybdates are quite limited.⁹ Oxide-based nanomaterials are interesting because of their robustness and less toxicity.¹⁰ Among the various Ln^{3+} -doped oxide nanomaterials, water dispersible molybdates are less explored. Molybdate (MoO_4^{2-}) crystal has a tetrahedral symmetry (Td)

with the central Mo^{2+} metal ion coordinated by four O^{2-} ions. As one of the interesting inorganic functional materials, molybdates have attracted special attention because of their wide use in catalysis, luminescent materials, pigments, and so on.¹¹⁻¹⁶ Molybdate phosphors have broad and intense absorption bands due to charge transfer (CT) from oxygen to metal in the near-UV region.¹⁷⁻²¹ For example, trivalent rare earth molybdates phosphors, such as $\text{Y}_2(\text{MoO}_4)_3:\text{Eu}^{3+}$ and $\text{Gd}_2(\text{MoO}_4)_3:\text{Dy}^{3+}$, have been investigated because they are good hosts for red and green emitting phosphors for solid-state lighting based on InGaN diodes.²²⁻²⁷ Not only, Ln-based molybdates but alkali metal molybdates²⁸⁻³¹ are interesting due to the ionic size of the alkali metals close to Ln^{3+} ions. Among the MMoO_4 ($\text{M} = (\text{Ca}^{2+}, \text{Ba}^{2+}, \text{Sr}^{2+}$ etc.), CaMoO_4 is attractive for the following reasons. First, CaMoO_4 is highly transparent material to allow a wide range of light to pass through without much attenuation in luminescence. Second, CaMoO_4 is a robust phosphor due to its high density (4.25 g cm^{-3}) and possess better physical and chemical properties compared to other oxide materials. There have been quite a few reports on Stokes luminescence of Ln^{3+} -doped CaMoO_4 nanocrystals in the recent past.³²⁻³⁶ Ju et al. has reported the synthesis of $\text{CaMoO}_4:\text{Eu}^{3+}$ phosphor via sol-gel process. The quantum efficiency of this material is 20% higher than the one with solid state reaction.³⁷ Sharma et al. has achieved a series of CaMoO_4 phosphors doped with Dy^{3+} and co-doped with K^+ by hydrothermal method. They have performed photometric characterization of these nanocrystals which indicates the

suitability of this phosphors in commercial white LEDs and other display devices.³⁸ Apart from Stokes luminescence, there are some reports available on upconversion luminescence of Ln³⁺-doped CaMoO₄ nanomaterials.³⁹ Ryu et al. has reported controllable white upconversion luminescence in Ho³⁺/Yb³⁺/Tm³⁺-doped CaMoO₄ nanocrystals synthesized using a complex citrate-gel method.⁴⁰ The same group has shown green upconversion luminescence from polycrystalline Er³⁺/Yb³⁺-co doped CaMoO₄ nanocrystals and also the effect of Li⁺ doping to the enhancement of green UC emission.⁴¹ However, most of these reports are discussed on solid state materials. To fully explore the potential application of molybdates, it would be highly desirable to downscale their sizes to the nanoregime to expand their potential for various applications.

In this article, we report the synthesis of water dispersible Eu³⁺-doped CaMoO₄ nanocrystals under microwave condition. The water dispersibility is achieved with a thin coating of sodium dodecyl sulphate (SDS) over the Ln³⁺-doped CaMoO₄ surface. The optimum concentration of Eu³⁺ is 5mol% leading to very intense luminescence signal in water. This led to the enhanced Eu³⁺ luminescence quantum efficiency close to 40% in CaMoO₄ nanocrystals. Under 980 excitation, Er³⁺/Yb³⁺-doped CaMoO₄ nanocrystals show a strong peak close to 833 nm in the NIR region which to our knowledge is rarely reported.⁴² Furthermore, the nanocrystals display strong photocatalytic activity which is verified through the degradation of Rhodamine B (RhB) dye. We observed an 80% degradation of RhB under UV illumination which is close to that reported for ZnO. The high luminescence quantum efficiency and strong photocatalytic properties of Ln³⁺-doped CaMoO₄ nanocrystals make them suitable materials for dual applications.

2 Experimental sections:

2.1 Materials: Eu₂O₃, Er₂O₃, Yb₂O₃ (from Sigma-Aldrich), ammonium heptamolybdate tetra hydrate [(NH₄)₆Mo₇O₂₄·4H₂O], CaCl₂ (from Merck), deionized water, 1 (M) HNO₃ (Merck, 70% pure), sodium dodecyl sulphate (SDS) were purchased from Merck. All chemicals were used without further purification.

2.2 Synthesis:

Water dispersible Eu³⁺-doped CaMoO₄ nanocrystals were synthesized using a microwave (MW) procedure. Briefly, the stoichiometric amounts of Eu₂O₃ was converted into their corresponding nitrate by dissolving in 1 M HNO₃ whereas CaCl₂, (NH₄)₆Mo₇O₂₄·4H₂O and SDS were used as received. In a typical procedure, (NH₄)₆Mo₇O₂₄·4H₂O/H₂O stock solution was prepared by dissolving 1 mmol (NH₄)₆Mo₇O₂₄·4H₂O in 25 ml H₂O at room temperature. A mixture of CaCl₂ (0.95 mmol, 105.44 mg), Eu(NO₃)₃ (0.05 mmol, 16.9 mg), SDS (1 mmol, 288.38 mg) and 15 ml H₂O was heated to about 60° C under vigorous stirring, forming a transparent solution. A 2 ml from the (NH₄)₆Mo₇O₂₄·4H₂O/H₂O stock solution was slowly added into the mixture and stirring was continued for another 10 min. Subsequently the transparent solution was transferred to a 10 ml vial used for microwave synthesis and placed in the microwave reactor (Anton Paar Monowave 300). The vial was tightly sealed with Teflon cap and then microwave heated at 90° C for 10 minutes. Finally, the white coloured product appeared as a precipitate was collected by centrifugation and washed thrice with ethanol, followed by deionized water to

remove any unreacted reactants. For Er³⁺/Yb³⁺-doped CaMoO₄ the same protocol was followed, except the use of Er(NO₃)₃ and Yb(NO₃)₃ instead of Eu(NO₃)₃.

2.3 Characterization:

The XRD patterns were collected using the Rigaku-SmartLab diffractometer attached with D/tex ultra detector and Cu K_α source operating at 35 mA and 70 kV. Scan range was set from 10-70° 2θ with a step size of 0.02° and a count time of 2 sec. The samples were well powdered and spread evenly on a quartz slide. Field emission scanning electron microscopy (FESEM) images were taken on the SUPRA 55-VP instrument with patented GEMINI column technology. Prior to loading of the samples into the chamber, they were coated with a thin film of gold-palladium in order to avoid charging effects. TEM images were taken on a UHR-FEG-TEM, JEOL; JEM 2100 F model using a 200 kV electron source. Samples were prepared by placing a drop of aqueous dispersion of the nanocrystals on a carbon coated copper grid and the grid was dried under air. Thermogravimetric analysis was performed using Mettler Toledo TGA 851 instrument under N₂ atmosphere at a heating rate of 10° min⁻¹. Room temperature optical absorption spectra of all the samples were recorded on a Hitachi U4100 spectrophotometer. The samples were taken in a 3 ml quartz cuvette (path length, 1 cm). The PL spectra were measured on a Horiba Jobin Yvon spectrometer equipped with 450 W Xe lamp. The excitation and emission light were dispersed using Czerny-Turner monochromator with an optical resolution of 1 nm. The emitted photons were detected using a Hamamatsu R928 detector. The output signal was recorded using a computer. For the upconversion measurements, the nanocrystals dispersion was excited with a 980 nm diode laser from RgBLase LLC, which was coupled with a fibre with a core diameter of 100 μm. The output signal was measured using Jobin Yvon spectrometer. The PL lifetime measurements were performed with the Horiba Jobin Yvon Fluorolog CP machine equipped with a pulsed Xe source operating at 25 W.

3 Results and Discussion:

The microwave method used for the synthesis of SDS capped Ln³⁺-doped CaMoO₄ [Ln³⁺ = Eu³⁺, Er³⁺/Yb³⁺] nanocrystals led to the formation of water dispersible nanocrystals in the size range of 100 nm. The high water dispersibility suggests that SDS coating is in the form of bilayer. This is confirmed from the luminescence studies (*vide infra*). These nanocrystals are quite monodispersed and spherical in shape as confirmed from HR-TEM image shown in Fig. 1. The high monodispersity in the size is further substantiated by the narrow distribution obtained with DLS measurements (Fig. 1B). The hydrodynamic size of the nanocrystals obtained from the DLS

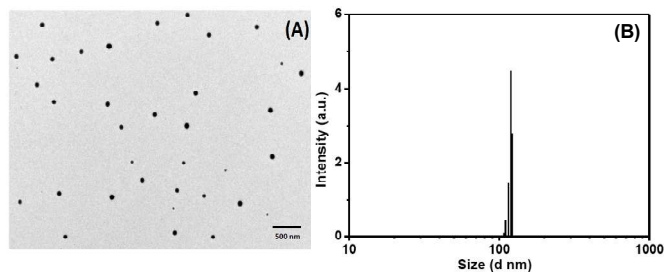


Fig. 1. TEM image (A) and particle size distribution from DLS (B) of water dispersed CaMoO₄:Eu³⁺ nanocrystals indicating the formation of monodispersed nanocrystals.

measurements is about 120 nm. This is also supported by SEM images shown in Fig. S1 in the supporting information. Formation of pure tetragonal phase CaMoO_4 nanocrystals is verified from the XRD patterns shown in Fig. 2. The observed diffraction peaks matched very well with the standard pattern of tetragonal phase

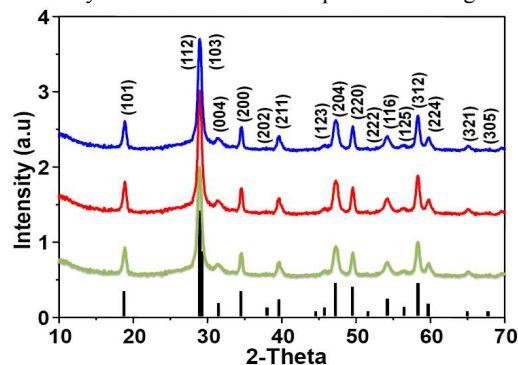


Fig. 2 XRD patterns of CaMoO_4 nanocrystals (green) undoped, (red) Eu^{3+} -doped and (blue) $\text{Er}^{3+}/\text{Yb}^{3+}$ -doped and standard pattern (black).

CaMoO_4 (ICSD PDF Card No.: 01-085-1267). The strong diffraction peaks clearly indicate good crystallinity in the as-synthesized products. Absence of any additional peaks suggests that CaMoO_4 nanocrystals with high phase purity can be easily obtained through microwave synthetic method. The binding of SDS molecules to the surface of CaMoO_4 nanocrystals is confirmed by FTIR spectra shown in Fig. 3. Briefly, a broad band centered at 3350 cm^{-1} due to O–H stretching vibrations is observed. The C–H stretching vibrations of the methylene ($-\text{CH}_2$) units are observed near 2850 cm^{-1} and 2922 cm^{-1} . The region between 600 to 900 cm^{-1} is

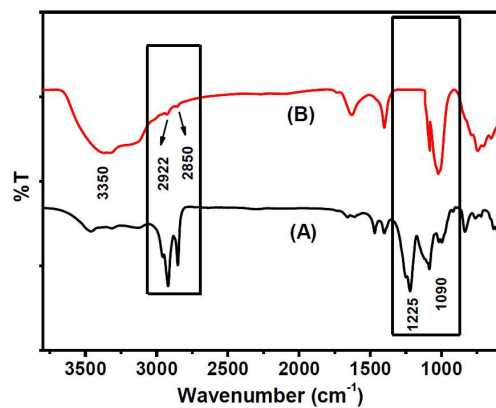


Fig. 3 FTIR spectra of (A) free SDS molecules (B) SDS capped nanocrystals in H_2O .

indicating the C–H bending frequencies of $-\text{CH}_2$ units. For the pure SDS two strong peaks were noted near 1090 cm^{-1} (symmetric stretching) and 1225 cm^{-1} (asymmetric stretching), which are assigned to the S=O groups of sulphate. These peaks shifted to lower energy as well as merged in the case of SDS coated nanocrystals indicating the binding of S=O groups of SDS to the nanocrystals. To further confirm the SDS coating onto the surface of CaMoO_4 nanocrystals, TGA analysis was conducted. The TGA curve for SDS coated CaMoO_4 and the free SDS are compared in Fig. S2. For the free SDS the major weight loss is noted from 168 to $350\text{ }^\circ\text{C}$ due to the decomposition of SDS molecules. For the SDS coated CaMoO_4 nanocrystal, the onset of decomposition is shifted to higher temperature ($220\text{ }^\circ\text{C}$). This substantiates the FTIR result that the SDS molecules are attached strongly to the CaMoO_4 surface. In

addition, the narrow decomposition range indicates that all the nanocrystals are more or less evenly coated with the SDS. The optical studies of SDS coated Eu^{3+} -doped CaMoO_4 nanocrystals show some interesting characteristics. Upon UV (394 nm) excitation, the nanocrystals emit strong emission near 614 nm as shown in Fig. 4 which is assigned to ${}^5\text{D}_0 \rightarrow {}^7\text{F}_2$ transition. In addition to the strong emission at 614 nm , there are less intense emission peaks observed

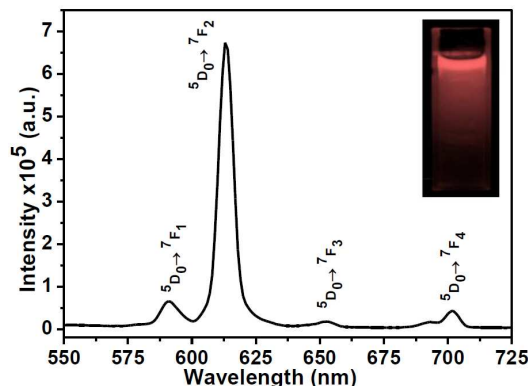


Fig. 4 Emission spectrum of SDS coated $0.1\text{ wt}\%$ Eu^{3+} -doped CaMoO_4 nanocrystals in water. Inset shows the digital image of the colloidal nanocrystals under 366 nm UV light.

near 590 , 650 and 700 nm . These peaks are respectively ascribed to ${}^5\text{D}_0 \rightarrow {}^7\text{F}_1$, ${}^5\text{D}_0 \rightarrow {}^7\text{F}_3$ and ${}^5\text{D}_0 \rightarrow {}^7\text{F}_4$ transitions. The ${}^5\text{D}_0 \rightarrow {}^7\text{F}_2$ transition being quite intense gives rise to the bright red light from $0.1\text{ wt}\%$ aqueous dispersion Eu^{3+} -doped CaMoO_4 nanocrystals (shown in the inset of Fig. 4). The ${}^5\text{D}_0 \rightarrow {}^7\text{F}_2$ emission is hypersensitive in nature and its intensity depends on the local crystallite environment around the Ln^{3+} ions. Intense ${}^5\text{D}_0 \rightarrow {}^7\text{F}_2$ transition is generally observed when Eu^{3+} ions are present in a non-centro symmetric environment. However, in CaMoO_4 , both Ca^{2+} and Mo^{2+} have S_4 point symmetry possessing an inversion centre. This suggests weaker emission intensity for ${}^5\text{D}_0 \rightarrow {}^7\text{F}_2$ transition. We believe that the observed strong emission might be due to nanocrystals possess some defects or disorderness leading to distortion in the symmetry sites where Eu^{3+} ions occupy. This is verified by preparing bulk Eu^{3+} -doped CaMoO_4 nanocrystals via sol-gel process. The material is heated at $800\text{ }^\circ\text{C}$ to achieve better crystallinity. For the bulk powder sample the asymmetric ratio ($614/591$) is 1.75 whereas for SDS coated nanocrystals the corresponding value is 7.75 suggesting the more distortions near crystals site of Eu^{3+} in the case of nanocrystals. The luminescence spectrum of the bulk material is shown in Fig. S3. Alternatively, we believe there can be an alternative reason such as polarization effect, which alters the crystal field strength as well as affects the transition probabilities. We have now modified our explanation based on the appropriate reports and the same is included in the reference.^{36a, 43}

The luminescence lifetime of the ${}^5\text{D}_0$ state of Eu^{3+} ion in SDS coated $\text{CaMoO}_4:\text{Eu}^{3+}$ -doped nanocrystals is about 2.16 ms as calculated from the decay analysis (shown in Fig. S4). The intense luminescence signal and longer lifetime of Eu^{3+} ion in $\text{CaMoO}_4:\text{Eu}^{3+}$ -doped nanocrystals is further supported by the quantum efficiency of the nanocrystals in aqueous medium. The calculated quantum yield is about 40% which is measured using quinine sulphate as the reference standard. The details of the measurement and the calculations are given in Fig. S5. This value is higher than the calculated 15% for $\text{YVO}_4:\text{Eu}^{3+}$ (5%) colloidal nanocrystals.⁴⁴ Haase et al. reported a luminescence quantum yield equal to 38% for colloidal $\text{YVO}_4:\text{Eu}^{3+}$ (15%) nanocrystals with an average size of 30 nm at room temperature.⁴⁵ The above points clearly suggest that SDS coated $\text{CaMoO}_4:\text{Eu}^{3+}$ (5%) nanocrystals are

better matrix for Eu^{3+} ions. To our knowledge there are only very few reports with high quantum yield for Eu^{3+} ion in water. To understand the reason for increased quantum efficiency for Eu^{3+} ions in CaMoO_4 nanocrystals we prepared Eu^{3+} -doped CaMoO_4 nanocrystals without SDS coating under identical condition. The observed life time for the Eu^{3+} ion is 1.93 ms, which is lower compared to the SDS coated CaMoO_4 nanocrystals (Fig. S6). This implies that one of the reasons for the enhanced quantum efficiency for Eu^{3+} ion in CaMoO_4 matrix is the strong SDS coating that can probably reduce the number of defects near the surface of the nanocrystals.

The high water dispersibility of the nanocrystals after SDS coating suggests that SDS is mostly in the form of bilayer, thus SO_3^- on the surface of the nanocrystals. The bilayer formation is further verified by the slow addition of toluene to the water dispersible nanocrystals which upon slight sonication led to the nanocrystals move to the toluene phase. This phase transfer is supported by the strong Eu^{3+} emission from nanocrystals dispersed in toluene (shown in Fig. S7). This is interesting that the nanocrystals can be used both in organic and aqueous phase without additional surface chemistry.

The luminescence studies were extended to understand the upconverting ability of the CaMoO_4 nanocrystal by doping $\text{Er}^{3+}/\text{Yb}^{3+}$ ions. Due to high absorption coefficient Yb^{3+} ions are used as sensitizer in the upconversion process. Moreover, it has only one excited electronic state ($^2\text{F}_{5/2}$) which is matching with the 980 nm excitation wavelength. The nanocrystals in H_2O showed a weak emission whereas in toluene they exhibit intense upconversion emission which is shown in Fig. 5. The green emission peaks centered at 530 and 550 nm are assigned to the $^2\text{H}_{11/2} \rightarrow ^4\text{I}_{15/2}$ and $^4\text{S}_{3/2} \rightarrow ^4\text{I}_{15/2}$ transitions, respectively.

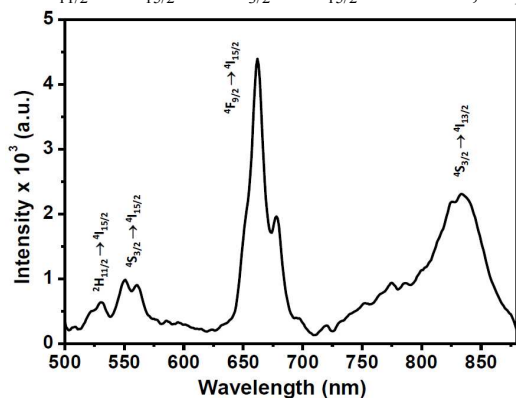


Fig. 5 Upconversion emission spectrum of SDS coated $\text{Er}^{3+}/\text{Yb}^{3+}$ -doped CaMoO_4 nanocrystals in toluene measured by exciting the sample with a 980 nm diode laser at 400 mW laser powers.

The other emission peak at 668 nm is assigned to the $^4\text{F}_{9/2} \rightarrow ^4\text{I}_{15/2}$ transition. It is interesting to note that along with the characteristic green and red emission peaks, the nanocrystals exhibit a relatively strong peak close to 833 nm in the NIR region. This peak is assigned to $^4\text{I}_{9/2} \rightarrow ^4\text{I}_{15/2}$ transition. To the best of our knowledge, this NIR emission peak is less reported in the literature. To investigate the origin of this peak, we prepared CaMoO_4 nanocrystals doped with Er^{3+} and Yb^{3+} independently using similar synthetic protocol. Hardly any emission was observed from both the samples upon exciting with 980 nm. These results suggest the absence of excited state absorption as well as scattering of light from Yb^{3+} ions in nanocrystals. The results are shown in Fig. S8. To understand the mechanism responsible for the UC emission observed above, we prepared $\text{CaMoO}_4:\text{Yb}^{3+}/\text{Er}^{3+}$ nanocrystals without

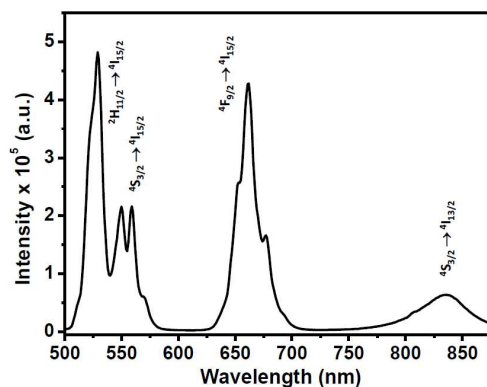


Fig. 6 Upconversion emission spectrum of $\text{Er}^{3+}/\text{Yb}^{3+}$ -doped CaMoO_4 nanocrystals (without SDS coating) measured by exciting the sample with a 980 nm diode laser operating at 400 mW laser power.

SDS coating. The UC emission spectrum of this sample shown in Fig. 6 is quite different from the same obtained with SDS coated nanocrystals. A very strong green UC emission is

observed for the nanocrystals prepared without SDS coating. For the SDS-coated nanocrystals, the intensity ratio $I_{\text{NIR}}/I_{\text{red}}$ is about 1.40 whereas the corresponding value is only 0.38 for nanocrystals without SDS coating. These results suggest that the NIR emission is probably associated with surface properties of the nanocrystals. The number of photons involved in the energy transfer process is understood by doing the power dependent studies as the laser power, $P \propto I^n$, where I is the intensity of the upconversion emission and n is the number of photons involved in generating the upconversion emission. A logarithmic plot of the laser power against the emission intensity gives a slope of n . As shown in Fig. S9 and S10, the slopes (n) of the plots are 1.89 and 2.46 for the red and NIR emissions, respectively. Based on the above results we propose the following mechanism which is schematically shown in Fig. 7. First, Er^{3+} in the ground state is excited to $^4\text{I}_{11/2}$ via energy

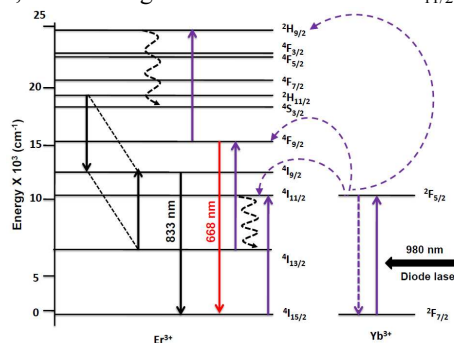


Figure 7. Upconversion mechanism for $\text{Er}^{3+}/\text{Yb}^{3+}$ -doped CaMoO_4 nanocrystals prepared via microwave method.

transfer (ET) from Yb^{3+} ions. Because of the short lifetime of $^4\text{I}_{11/2}$ state most of ions will non-radiatively decay and populate the $^4\text{I}_{13/2}$ state. The second energy transfer will excite the Er^{3+} and populate the $^4\text{F}_{9/2}$ state. The red emission occurs from this level. In addition, some of the excited Er^{3+} ions are excited further up in the energy to the $^2\text{H}_{9/2}$ state via the third energy transfer. Due to presence of energy levels which are close enough, the excited Er^{3+} ions reach $^2\text{H}_{11/2}/^4\text{S}_{3/2}$ non-radiatively. We propose the following cross-relaxation ($^2\text{H}_{11/2}/^4\text{S}_{3/2}, ^4\text{I}_{13/2}$) \rightarrow ($^4\text{I}_{9/2}, ^4\text{I}_{9/2}$) to occur at this stage thus populating the $^4\text{I}_{9/2}$ state. In the absence of such a cross-relaxation, intense green

emissions are excepted from ${}^2H_{11/2}/{}^4S_{3/2}$ states. Though the reason for the cross-relaxation is not clear, but we presume that SDS ligands might have a role.

Finally, we have extended the study to investigate the photocatalytic activity of CaMoO_4 nanocrystals. The photocatalytic activity of PbMoO_4 and BiVO_4 with scheelite structure has been reported.^{46,47} To the best of our knowledge, there is no report on the photocatalytic activity of CaMoO_4 nanocrystals. Because of the relatively high band gap energy of CaMoO_4 ($E_g = 3.41$ eV), the molybdate was tested as a photocatalyst under UV irradiation. The conduction band of CaMoO_4 is located above the RhB redox potential ($E_{\text{RhB}^+/\text{RhB}}^0 = 1.34$ eV) versus standard calomel electrode (SCE), allowing CaMoO_4 to be catalytically active. We believe that reactive oxygen species (e.g., HO^\cdot , $\text{O}_2^{\cdot-}$ etc), especially HO^\cdot radicals can oxidize the organic dye molecules and perform photocatalysis. The Rhodamine B (RhB) dye degradation was demonstrated over the surface of CaMoO_4 nanocrystals under UV illumination to elucidate the photocatalytic activity. To get good adsorption of the dye to the nanocrystals surface, the photocatalytic property was studied without SDS coating. Fig. 8 shows that RhB dye is significantly degraded by ~80% under UV illumination within 4 hours. The pie chart diagram of RhB dye degradation (see Fig. S11) reveals that over half the concentration of the dyes is degraded in the first 120 minutes.

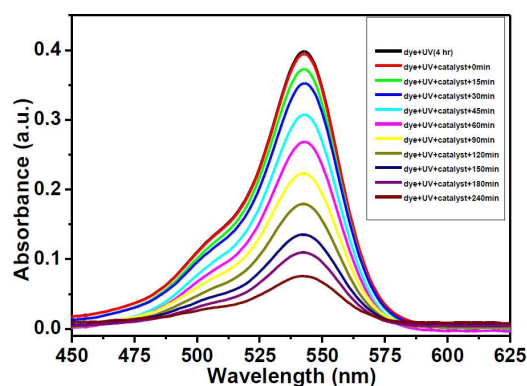


Fig. 8 UV-Vis spectra of RhB dye as function of time over CaMoO_4 nanocrystals.

The RhB dye degradation follows apparent first order kinetics in agreement with a general Langmuir–Hinshelwood mechanism;

$$r = -dC/dt = k_1 k_2 C / (1 + k_2 C)$$

where, r is the degradation rate of the dye (mg/min), C the concentration of the dye (mg/lit), t the illumination time, k_2 the adsorption coefficient of dye (1/mg), and k_1 is the reaction rate constant (mg/min). If C is very small then the above equation could be simplified to

$$\ln(C_0/C) = k_1 k_2 t = kt$$

where C_0 is the initial concentration of the dye, C is the concentration of the dye after certain time t with UV illumination, k is the rate constant and t is the certain time. A plot of $\ln(C_0/C)$ Vs t (shown in Fig. S12) provides a slope value 0.0274 min^{-1} , which is nothing but the rate constant (k) of dye degradation by CaMoO_4 nanocrystals in the photocatalysis process. It is interesting to note that the resulting value is comparable with the reported value for ZnO photocatalyst.⁴⁸

Conclusions

In this article we have reported the microwave synthesis of sodium dodecyl sulphate coated Ln^{3+} -doped CaMoO_4 nanocrystals ($\text{Ln}^{3+} =$

Eu^{3+} , $\text{Er}^{3+}/\text{Yb}^{3+}$). SEM and TEM measurements suggest the average size of the nanocrystals to be 100 nm. FTIR and TGA analyses confirm that SDS binds strongly to the nanocrystals. The high water dispersibility of the nanocrystals after SDS coating suggests that SDS coating is in the form of bilayer. Upon UV excitation, the Eu^{3+} -doped CaMoO_4 nanocrystals show strong red emission characteristics of Eu^{3+} ions with a high quantum efficiency close to 40%. Under 980 excitation, $\text{Er}^{3+}/\text{Yb}^{3+}$ -doped CaMoO_4 nanocrystals exhibit upconversion luminescence in toluene. In addition, the nanocrystals show strong photocatalytic activity which is verified from the RhB dye degradation under UV illumination. The high quantum efficiency and water dispersibility of Ln^{3+} -doped CaMoO_4 nanocrystals can be used as potential materials for dual applications.

Acknowledgements

VM thanks the Department of Science and Technology (DST) India, CSIR and IISER-Kolkata for the funding. CH and TS thank IISER-Kolkata and UGC respectively for their scholarship.

Notes and references

^a Department of Chemical Sciences, Indian Institute of Science Education and Research (IISER), Kolkata, Mohanpur, West Bengal 741252, India.

Fax: 91-33-25873020; Tel: +91(0)9007603474;

E-mail: mvenkataramanan@yahoo.com

† Electronic Supplementary Information (ESI) available SEM, DLS, TGA, PL in toluene, solid state PL, Life time, Quantum yield, UC of $\text{CaMoO}_4:\text{Er}^{3+}$ and $\text{CaMoO}_4:\text{Yb}^{3+}$ NCs, UC power dependence study, pie chart diagram and Photocatalysis kinetics. See DOI: 10.1039/b000000x/

1 (a) A. J. Steckl, M. Garter, D. S. Lee, J. Heikenfeld and R. Birkhahn, *Appl. Phys. Lett.*, 1999, **75**, 2184; (b) J. H. Kim and P. H. Holloway, *Adv.Mater.*, 2005, **17**, 91;

2 (a) F. Auzel, *Chem. Rev.*, 2004, **104**, 139; (b) S. Sivakumar, F. C. J.M. van Veggel and M. Raudsepp, *J. Am. Chem. Soc.*, 2005, **127**, 12464; (c) S. Heer, O. Lehmann, M. Haase and H.-U. Güdel, *Angew. Chem., Int. Ed.*, 2003, **42**, 3179; (d) M. Haase and H. Schäfer, *Angew. Chem., Int. Ed.*, 2011, **50**, 5808; (e) F. Wang and X. Liu, *J. Am. Chem. Soc.*, 2008, **130**, 5642; (f) C. Li and J. Lin, *J. Mater. Chem.*, 2010, **20**, 6831; (g) S. Cotton, *Lanthanide and Actinide Chemistry*, John Wiley & Sons, West Sussex, 2006; (h) C.G.Bunzli, *Chem. Rev.*, 2002, **102**, 1897; (i) F. Wang, Y. Han, C. S. Lim, Y. Lu, J. Wang, J. Xu, H. Chen, C. Zhang, M. Hong and X. Liu, *Nature*, 2010, **463**, 1061; (j) V. Sudarsan, F. C. J. M. Van Veggel, R. A. Herring and M. Raudsepp, *J. Mater. Chem.*, 2005, **15**, 1332

3 (a) G. Blasse and B. C. Grabmaier, *Luminescent Materials*, Springer, Berlin, 1994; (b) A. Kitai, *Luminescent Materials and Applications*, John Wiley & Sons, West Sussex, 2008, ; (c) C. R. Ronda, T. Justel and H. Nikol, *J. Alloys Compd.*, 1998, **275–277**, 669; (d) T. Montini, A. Speghini, L. De Rogatis, B. Lorenzut, M. Bettinelli, M. Graziani and P. Fornasiero, *J. Am. Chem. Soc.*, 2009, **131**, 13155.

4 (a) V. Mahalingam, M. Francesca, F. Vetrone, V. Venkatramu, A. Speghini, M. Bettinelli and J. A. Capobianco, *J. Phys. Chem. C*, 2008, **112**, 17745; (b) J. Silver, E. Barrett, P. J. Marsh and R. J. Withnall, *J. Phys. Chem. B*, 2003, **107**, 9236; (c) F. Pandozzi, F. Vetrone, J.-C. Boyer, R. Naccache, J. A. Capobianco, A. Speghini and M. A. Bettinelli, *J. Phys. Chem. B*, 2005, **109**, 17400; (d) J. Silver, M. I. Martinez-Rubio, T. G. Ireland, G. R. Fern and R. Withnall, *J. Phys. Chem. B*, 2001, **105**, 948; (e) H. Schafer, P. Ptacek, K. Kömpe and M. Haase, *Chem. Mater.*, 2007, **19**, 1396; (f) D. Chen, Y. Yu, F. Huang, P. Huang, A. Yang and Y. Wang, *J. Am. Chem. Soc.*, 2010, **132**, 9976; (g) X. Zhang, P. Yang, C. Li, D. Wang, J. Xu, S. Gai and J. Lin, *Chem. Commun.*, 2011, **47**, 12143; (h) N. J. J. Johnson, N. M. Sangeetha, J. C. Boyer and F. C. J. M. Van Veggel, *Nanoscale*, 2010, **2**, 771; (i) J. Pichaandi, F. C. J. M. Van Veggel and M. Raudsepp, *ACS Appl. Mater. Interfaces*, 2010, **2**, 157

- 5 (a) D. E. Achatz, A. Rehmand, O. S. Wolfbeis, *Top. Curr. Chem.*, 2011, **300**, 29; (b) S.M. Saleh, R. Aliand O.S. Wolfbeis, *Chem.Eur. J.*, 2011, **17**, 14611; (c) N. Bogdan, E. M. Rodríguez, F. S. Rodríguez, M. C. I. de la Cruz, A. Juarranz, D. Jaque, J. G. Solé and J. A. Capobianco, *Nanoscale*, 2012, **4**, 3647; (d) G. Y. Chen, T. Y. Ohulchaskyy, W. Law, H. Agren and P. N. Prasad, *Nanoscale*, 2011, **3**, 2003; (e) S. Sarkar, C. Hazra, M. Chatti, V. Sudarsan and V. Mahalingam, *RSC Adv.*, 2012, **2**, 8272.
- 6 (a) H. Q. Wang and T. Nann, *ACS Nano*, 2009, **3**, 3804; (b) V. Mahalingam, F. Vetrone, R. Naccache, A. Speghini and J. A. Capobianco, *J. Mater. Chem.*, 2009, **19**, 3149; (c) S. Sarkar, C. Hazra and V. Mahalingam, *Dalton Trans.*, 2013, **42**, 63; (d) W. Quan, D. M. Yang, P. P. Yang, X. M. Zhang, H. Z. Lian, X. M. Liu and J. Lin, *Inorg. Chem.*, 2008, **47**, 9509; (e) S. Sarkar, C. Hazra and V. Mahalingam, *Chem.Eur. J.*, 2012, **18**, 7054; (f) S. Sarkar, B. Messaragandla, C. Hazra and V. Mahalingam, *Adv. Mater.* 2013, **25**, 860; (g) P. Rahman and M. Green, *Nanoscale*, 2009, **1**, 214.
- 7 (a) G. Wang, Q. Peng and Y. Li, *Acc. Chem. Res.*, 2011, **44**, 322; (b) X. Yu, M. Li, M. Xie, L. Chen, Y. Li and Q. Wang, *Nano Res.*, 2010, **3**, 51; (c) F. Wang and X. Liu, *J. Am. Chem. Soc.*, 2008, **130**, 5642; (d) L. Wang, P. Li and Y. Li, *Adv. Mater.*, 2007, **19**, 3304; (e) C. Zhang, Z. Hou, R. Chai, Z. Cheng, Z. Xu, C. Li, L. Huang and J. Lin, *J. Phys. Chem. C*, 2010, **114**, 6928; (f) H. P. Paudel, L. Zhong, K. Bayat, M. F. Baroughi, S. Smith, C. Lin, C. Jiang, M. Berry and S. May, *J. Phys. Chem. C*, 2011, **115**, 19028; (g) P. Ghosh, A. Kar and A. Patra, *J. Phys. Chem. C*, 2010, **114**, 715; (h) D. Yang, Y. Dai, P. Ma, X. Kang, M. Shang, Z. Cheng, C. Li and J. Lin, *J. Mater. Chem.*, 2012, **22**, 20618.
- 8 (a) S. Sarkar, C. Hazra and V. Mahalingam, *Dalton Trans.*, 2013, **42**, 63; (b) P. Ghosh, A. Kar and A. Patra, *Nanoscale*, 2010, **2**, 1196; (c) N. J. J. Johnson, A. Korinek, C. Dong and F. C. J. M. van Veggel, *J. Am. Chem. Soc.* 2012, **134**, 11068; (d) N. J. J. Johnson and F. C. J. M. Van Veggel, *Nano Res.* 2013, **6**, 547; (e) S. Li, X. Zhang, Z. Hou, Z. Cheng, P. Ma and J. Lin, *Nanoscale*, 2012, **4**, 5619; (f) X. Zhang, P. Yang, C. Li, D. Wang, J. Xu, S. Gai and J. Lin, *Chem. Commun.*, 2011, **47**, 12143; (g) C. Li, Z. Xu, D. Yang, Z. Cheng, Z. Hou, P. Ma, H. Lian and J. Lin, *Cryst.Eng.Comm.* 2012, **14**, 670.
- 9 (a) H. Chen and J. Ren, *Analyst*, 2012, **137**, 1899; (b) C. Hazra and V. Mahalingam, *RSC Adv.*, 2013, **3**, 9200; (c) Y. C. Chen, Y. C. Wu, D. Y. Wang and T. M. Chen, *J. Mater. Chem.*, 2012, **22**, 7961; (d) A. Huignard, T. Gacoïn and J. P. Boilot, *Chem. Mater.* 2000, **12**, 1090; (e) G. Mialon, M. Gohin, T. Gacoïn, J. P. Boilot, *ACS Nano*, 2008, **2**, 2505; (f) Z. Hu, M. Ahrén, L. Selegard, C. Skoglund, F. Söderlind, M. Engström, X. Zhang and K. Uvdal, *Chem. Eur. J.*, 2013, **19**, 12658; (g) M. Darbandi, W. Hoheisel and T. Nann, *Nanotechnology*, 2006, **17**, 4168; (h) Y. Sun, H. Liu, X. Wang, X. Kong and H. Zhang, *Chem. Mater.*, 2006, **18**, 2726; (i) G. Mialon, S. Türkcan, G. Dantelle, D. P. Collins, M. Hadjipanayi, R. A. Taylor, T. Gacoïn, A. Alexandrou and J. P. Boilot, *J. Phys. Chem. C* 2010, **114**, 22449.
- 10 (a) A. Kar, A. Datta and A. Patra, *J. Mater. Chem.* 2010, **20**, 916; (f) C. Hazra, S. Sarkar, B. Meesaragandla and V. Mahalingam, *Dalton Trans.*, 2013, **42**, 11981; (b) Y. Wang, P. Yang, P. Ma, F. Qu, S. Gai, Y. Dai, N. Niu, F. He and J. Lin, *J. Mater. Chem. B*, 2013, **1**, 2056; (c) Y. Zhang, D. Geng, M. Shang, X. Zhang, X. Li, Z. Cheng, H. Lian and J. Lin, *Dalton Trans.*, 2013, **42**, 4799; (d) L. Perelshtein, E. Ruderman, N. Perkas, T. Tzanov, J. Beddow, E. Joyce, T. J. Mason, M. Blanes, K. Molla, A. Patlolla, A. I. Frenkel and A. Gedanken, *J. Mater. Chem. B*, 2013, **1**, 1968; (e) L. Perelshtein, E. Ruderman, N. Perkas, K. Traeger, T. Tzanov, J. Beddow, E. Joyce, T. J. Mason, M. Blanes, K. Molla and A. Gedanken, *J. Mater. Chem.*, 2012, **22**, 10736; (f) N. M. Sangeetha and F. C. J. M. van Veggel *J. Phys. Chem. C*, 2009, **113**, 14702; (g) J. W. Stouwdam, M. Raudsepp and F. C. J. M. Van Veggel, *Langmuir*, 2005, **21**, 7003; (h) K. K. Upendra, K. Linganna, S. B. Surendra, F. Piccinelli, A. Speghini, M. Giarola, G. Mariotto and C. K. Jayasankar, *Sci. Adv. Mater.*, 2012, **4**, 584; (i) D. Hreniak, J. Doskocz, P. Gluchowski, R. Liciecki, W. Sterk, N. Vu, D. X. Loc, T. K. Anh, M. Bettinelli and A. Speghini, *J. Lumin.*, 2011, **131**, 473; (j) Y. Koltypin, S. I. Nikitenko and A. Gedanken, *J. Mater. Chem.*, 2002, **12**, 1107; (k) P. Jeevanandam, Y. Diamant, M. Motiei and A. Gedanken, *Phys. Chem. Chem. Phys.*, 2001, **3**, 4107.
- 11 C. Mazzocchia, C. Aboumrad, C. Diagne, E. Tempesti, J. M. Herrmann and G. Thomas, *Catal. Lett.*, 1991, **10**, 181.
- 12 D. Spassky, S. Ivanov, I. Kitaeva, V. Kolobanov, V. Mikhailin, L. Ivleva and I. Voronina, *Phys. Status Solidi C*, 2005, **2**, 65.
- 13 H. Barry, F. Moore and D. Robitaille, *US Pat.*, 3 726 694, 1973.
- 14 S. S. Kim, S. Ogura, H. Ikuta, Y. Uchimoto and M. Wakihara, *Chem. Lett.*, 2001, **30**, 760.
- 15 R. Sundaram and K. S. Nagaraja, *Sens. Actuators, B*, 2004, **101**, 353.
- 16 Y. Li, G. Wang, K. Pan, Y. Qu, S. Liu and L. Feng, *Dalton Trans.*, 2013, **42**, 3366.
- 17 H. Wu, Y. Hu, W. Zhang, F. Kang, N. Li and G. Ju, *J. Sol-Gel Sci. Technol.* 2012, **62**, 233.
- 18 A. Xie, X. Yuan, S. Hai, J. Wang, F. Wang and L. Li, *J. Phys. D: Appl. Phys.* 2009, **42**, 105107.
- 19 Z. H. Zhang, Q. Huang, X. Zhao and Z. L. Huang, *Phys. Status Solidi A*, 2009, **206**, 2843;
- 20 X. Li, Z. Yang, L. Guan, J. Guo, Y. Wang and Q. Guo, *J. Alloys Compd.*, 2009, **478**, 686;
- 21 (a) S. I. Woo, J. S. Kim and H. K. Jun, *J. Phys. Chem. B*, 2004, **108**, 8946; (b) M. S. Vukosovich and J. P. G. Farr, *Polyhedron*, 1986, **5**, 559.
- 22 Y. S. Cho, Y. D. Huh, *Bull. Korean Chem. Soc.*, 2011, **32**, 1353.
- 23 Y. Tian, X. Qi, X. Wu, R. Hua and B. Chen, *J. Phys. Chem. C*, 2009, **113**, 10767.
- 24 Q. M. Wang and B. Wang, *Mater. Chem. Phys.* 2005, **94**, 241.
- 25 X. Zhao, X. Wang, B. Chen, Q. Meng, B. Yan and W. Di, *Opt. Mater.* 2007, **29**, 1680.
- 26 C. Guo, T. Chen, L. Luan, W. Zhang and D. Huang, *J. Phys. Chem. Solids*, 2008, **69**, 1905.
- 27 J. Wan, L. Chen, J. Sun, H. Zhong, X. Li, W. Lu, Y. Tian, H. Lin and B. Chen, *J. Alloys Compd.* 2010, **496**, 331.
- 28 P. J. Gellings and H. J. M. Bouwmeester, *Catalysis Today*, 1992, **12**, 105.
- 29 M. T. Le, M. Kovanda, V. Myslik, M. Vrnata, I. D. Van and S. Hoste, *Thin Solid Films*, 2006, **497**, 291.
- 30 L. T. sim, C. K. Lee and A. R. West, *J. Mater. Chem.* 2002, **12**, 19.
- 31 S. Bhattacharya and A. Ghosh, *J. Appl. Phys.* 2006, **100**, 114119.
- 32 (a) E. Cavalli, P. Boutinaud, R. Mahiou, M. Bettinelli and P. Dorenbos, *Inorg. Chem.* 2010, **49**, 4916; (b) Z. Hou, H. Chai, M. Zhang, C. Zhang, P. Chong, Z. Xu, G. Li, and J. Lin *Langmuir* 2009, **25**, 12340
- 33 (a) G. Li, Z. Wang, Z. Quan, C. Li and J. Lin, *J. Cryst. Growth Des.* 2007, **7**, 1797; (b) A. K. Parchur, A. I. Prasad, A. A. Ansari, S. B. Rai and R. S. Ningthoujam *Dalton Trans.*, 2012, **41**, 11032; (c) B. P. Singh, A. K. Parchur, R. S. Ningthoujam, A. A. Ansari, P. Singh and S. B. Rai, *Dalton Trans.*, 10.1039/C3DT52786G
- 34 F. Lei and B. Yan, *J. Solid State Chem.* 2008, **181**, 855.
- 35 X. Li, Z. Yang, L. Guan and Q. Guo, *Mater. Lett.* 2009, **63**, 1096.
- 36 (a) A. K. Parchur, R. S. Ningthoujam, S. B. Rai, G. C. Okram, R. A. Sing, M. Taygi, S. C. Gadkari, R. Tewari and R. K. Vatsa, *Dalton Trans.*, 2011, **40**, 7595; (b) A. K. Parchur, R. S. Ningthoujam, *Dalton Trans.*, 2011, **40**, 7590.
- 37 H. Wu, Y. Hu, W. Zhang, F. Kang, N. Li and G. Ju, *J Sol-Gel Sci Technol.*, 2012, **62**, 227.
- 38 S. Dutta, s. Som and S. K. Sharma, *Dalton, Trans.*, In Press.
- 39 C. S. Lim, *Journal of Ceram. Process. Res.* 2012, **13**, 825.
- 40 J. H. Chung, J. H. Ryu, S. W. Mhin, K. M. Kim and K. B. Shim, *J. Mater. Chem.* 2012, **22**, 3397.
- 41 J. H. Chung, J. H. Ryu, J. W. Eun, J. H. Lee, S. Y. Lee, T. H. Heo and K. B. shim, *Mater. Chem. Phys.* 2012, **134**, 695.
- 42 L. Wang, Y. Zhang and Y. Zhu, *Nano Res*, 2010, **3**, 317.
- 43 W. Wang, G. K. Liu, M. G. Brik, L. Seijo and D. Shi, *Phys. Rev. B: Condens. Matter Mater. Phys.*, 2009, **80**, 155120.
- 44 L. Li, M. Zhao, W. Tong, X. Guan, G. Li and L. Yang, *Nanotechnology* 2010, **21**, 195601 .
- 45 K. Riotzki and M. Hasse, *J. Phys. Chem. B*, 1998, **102**, 10129.
- 46 Z. Shan, Y. Wang, H. Ding and F. Huang, *J. Mol. Catal. A: Chem.* 2009, **302**, 54.
- 47 M. Shen, Q. Zhang, H. Chen and T. Peng, *Cryst. Eng. Comm.*, 2011, **13**, 2785.
- 48 Q. I. Rahman, M. Ahmad, S. K. Misra and M. Lohani, *Mater. Lett.*, 2013, **91**, 170.